Nr. 56
21. January 2019

universität innsbruck
Institut für Mathematik

Preprint-Series: Department of Mathematics - Applied Mathematics

Photoacoustic Tomography with Direction Dependent Data: An Exact Series Reconstruction Approach

G. Zangerl, S. Moon and M. Haltmeier

APPLIEDMATHEMATICS

Technikerstraße 13 - 6020 Innsbruck - Austria
Tel.: +43 512 507 53803 Fax: +43 512 507 53898
https://applied-math.uibk.ac.at

Photoacoustic Tomography with Direction Dependent Data: An Exact Series Reconstruction Approach

Gerhard Zangerl

Department of Mathematics, University of Innsbruck
Technikerstraße 13, 6020 Innsbruck, Austria
E-mail: gerhard.zangerl@uibk.ac.at

Sunghwan Moon

Department of Mathematics, College of Natural Sciences
Kyungpook National University, Daegu 41566, Republic of Korea
E-mail: sunghwan.moon@knu.ac.kr

Markus Haltmeier

Department of Mathematics, University of Innsbruck
Technikerstraße 13, 6020 Innsbruck, Austria
E-mail: markus.haltmeier}@uibk.ac.at

Abstract

In photoacoustic image reconstruction, it is commonly assumed that the acoustic pressure on the detection surface is given. However, this does not take into account that in a realistic scenario the detectors often have a certain directivity. In this case the actual data are more accurately described as a linear combination of the acoustic pressure and its normal derivative with respect to the measurement surface. In this paper, we will consider an inverse source problem for the wave equation for data that are a combination of acoustic pressure and its normal derivative. For the special case of a spherical detection geometry we are able to derive exact frequency domain reconstruction formulas. Numerical results show the robustness and validity of the derived inversion formula. We also derive an inversion formula for a weighted spherical mean transform.

Keywords: Photoacoustic tomography; spherical geometry; image reconstruction; wave equation; reconstruction formula; direction dependent data.

AMS subject classifications: 44A12, 65R32, 35L05, 92C55.

1 Introduction

Photoacoustic Tomography (PAT) is a hybrid imaging technique that combines high optical contrast and ultrasonic resolution. It is based on the generation of an ultrasound wave by a short laser pulse inside an object of interest. Thereby the initial

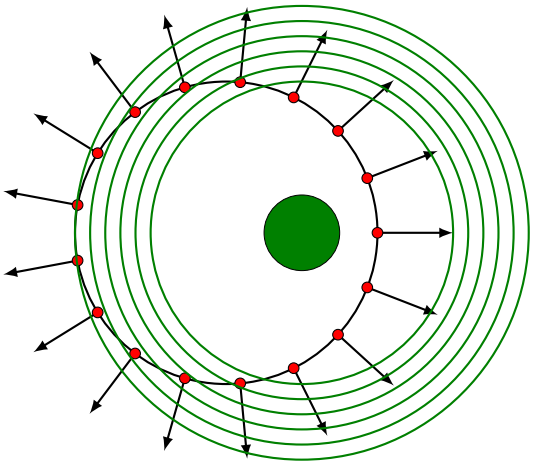

Figure 1: Pressure wave (green circles) emitted by an object (green disk) traversing a spherical measurement surface S (black circle). Each detector is displayed as red dot, which measures a combination of the pressure and its normal derivative.

pressure distribution of the sound wave encodes the electromagnetic absorption properties of the object, which are of great interest in medical diagnostics. PAT has proven to be very promising in medical areas like functional brain imaging of small animals, early cancer diagnostics and imaging of vasculature.

In a typical PAT setup the generated ultrasound wave propagates until it leaves the object and is then recorded by several point-like detectors. Typically, they are located on a surface S that (partially) encloses the volume Ω in which the object of interest is contained. In the standard PAT approach data collected in this way are identified with the restriction of the acoustic ultrasound wave to the surface S. In [1, 2] it is noted that measurements of standard detectors are direction dependent in the sense that they measure a combination of the pressure field and its normal derivative. Comparison of real data with numerically simulated direction dependent data also suggest this, see [1, 3]. In order to incorporate this direction dependency, the measurement of a detector located at $\mathbf{x} \in S$ measuring such a combination, see Figure 1, is modeled as

$$g(\mathbf{x}, t) = c_1 p(\mathbf{x}, t) + c_2 n(\mathbf{x}) \bullet \nabla_{\mathbf{x}} p(\mathbf{x}, t), \quad (\mathbf{x}, t) \in S \times [0, T],$$

where $n(\mathbf{x})$ denotes the outwards pointing normal of the surface at $\mathbf{x}$, T denotes the duration of the measurement and $c_1, c_2 \in \mathbb{R}$ are weight factors. For the first time we present PAT reconstructions based on such direction dependent data.

For the considered kind of data existing reconstruction algorithms can not be applied. For completeness, we mention important developments in PAT that can be adapted for the new data model: The classical problem in PAT consists in the reconstruction of the initial pressure distribution f, which corresponds to the case $c_2 = 0$ in our direction dependent data model. Many reconstruction methods for the desired initial pressure distribution have been derived in the recent years for various PAT situations. For example they include different detection geometries with variable or constant speed of sound or limited view situations. Also theoretical questions concerning uniqueness and stability of the inverse source problem were investigated [4–8]. A practically

important case for PAT reconstruction schemes assumes constant speed of sound wave propagation. Because of the simpler model in the constant sound speed case a vast number of explicit reconstruction formulas for f have been developed [9–17, 17–21] in the recent years. Among these formulas so called frequency domain reconstruction formulas provide very fast and accurate reconstructions. They give an expansion of the initial pressure f in terms of eigenfunctions of the Dirichlet or Neumann Laplacian Δ_Ω of the volume Ω. For special geometries, when the boundary of Ω is a sphere or a cylinder the eigenfunctions of Δ_Ω are explicitly known and thus lead to analytic reconstruction formulas [17–21].

In this work we will provide an explicit frequency domain reconstruction formula for direction dependent data that are based on an expansion of the spherical Laplace operator. Thereby we establish a relation between direction dependent data and the initial pressure distribution f. Reconstructions based on this formula are hard to implement directly due to possible divisions by zero. By using an expansion into a Fourier Bessel series, in Section 3 we derive an alternative formula that allows for a stable implementation. By expressing the direction dependent data in terms of a weighted spherical mean transform $M_{\cos}$ in Section 4 we also derive an inversion formula for $M_{\cos}$.

2 PAT with direction-dependent data

In PAT, sound propagation is commonly described by an acoustic pressure wave p that satisfies the initial value problem

$$\begin{aligned} \partial_t^2 p(\mathbf{x},t) - c(\mathbf{x})^2 \Delta_{\mathbf{x}} p(\mathbf{x},t) &= 0 && (\mathbf{x},t) \in \mathbb{R}^n \times [0,\infty), \\ p(\mathbf{x},0) &= f(\mathbf{x}) && \mathbf{x} \in \mathbb{R}^n, \\ \partial_t p(\mathbf{x},0) &= 0 && \mathbf{x} \in \mathbb{R}^n. \end{aligned} \tag{1}$$

In this work we assume that the speed of sound satisfies $c(\mathbf{x}) \equiv 1$ and that the initial pressure distribution satisfies $f \in C_0^\infty(\Omega)$. In PAT with direction dependent data we model measurement data as

$$g(\mathbf{x},t) = c_1 p(\mathbf{x},t) + c_2 n(\mathbf{x}) \cdot \nabla p(\mathbf{x},t), \quad (\mathbf{x},t) \in S \times [0,T]. \tag{2}$$

The aim of PAT with direction dependent data is to recover the initial pressure distribution f from g. To the best of or knowledge, this is a new inverse source problem for the wave equation that has not been considered so far. In the case when measurements are given by the normal derivative of the pressure ($c_1 = 0$) has been considered in [2, 22], wich gives an explicit inversion formula of the backprojection type when the detection surface is a sphere in three dimensions.

In this work, we will consider the case when the volume Ω is given by the $n-1$ dimensional ball B_{r_0} with radius r_0 centered at the origin. Our approach is based on Fourier space methods that lead to a relation between measurement data and the initial pressure distribution in the frequency domain. For the practical application the cases $n = 2$ and $n = 3$ are of relevance. In particular, the case $n = 2$ appears from direction dependent measurements with integrating line detectors on a cylindrical surface.

2.1 Exact inversion formula

The established relation between measurement data and initial pressure is stated in the frequency domain after applying several integral transforms. We denote the involved transforms by

$$\begin{aligned}
\mathcal{F}\{f\}(\boldsymbol{\xi}) &:= (2\pi)^{-\frac{n}{2}} \int_{\mathbb{R}^n} f(\mathbf{x}) e^{-i\mathbf{x}\cdot\boldsymbol{\xi}} d\mathbf{x}, \quad && \phi \in L^1(\mathbb{R}^n),\ \boldsymbol{\xi} \in \mathbb{R}^n \\
\mathcal{C}\{f\}(\lambda) &:= \int_0^\infty f(t)\cos(\lambda t) dt, && \phi \in L^1(0,\infty),\ \lambda > 0 \\
\mathcal{S}\{f\}(\lambda) &:= \int_0^\infty f(t)\sin(\lambda t) dt, && \phi \in L^1(0,\infty),\ \lambda > 0,
\end{aligned}$$

which are the Fourier, cosine and sine transform be defined on the spaces of absolutely integrable functions. Moreover, let $Y_{lk}(\boldsymbol{\theta})$ denote the spherical harmonic functions [23], which yield an expansion of the form

$$f(\rho\boldsymbol{\theta}) = \sum_{l=0}^{\infty} \sum_{k=0}^{N(n,l)} f_{lk}(\rho)\, Y_{lk}(\boldsymbol{\theta}),$$

$$\text{where } N(n,l) = \frac{(2l+n-2)(n+l-3)!}{l!(n-2)!} \quad \text{and} \quad N(n,0) = 1.$$

for any $f \in L^2\left(S^{n-1}\right)$.

In the following we derive a frequency domain reconstruction formula for the case of direction dependent data are

$$g(\boldsymbol{\theta}, t) = c_1 p(\boldsymbol{\theta}, t) + c_2 \boldsymbol{\theta} \bullet \nabla_{\mathbf{x}} p(\mathbf{x}, t)\big|_{\mathbf{x}=\boldsymbol{\theta}}, \quad (\boldsymbol{\theta}, t) \in S_{r_0}^{n-1} \times [0, T], \tag{3}$$

which is formula (2) for a spherical detection surface $S_{r_0}^{n-1} = \partial B_{r_0}$. We will also use the fact that a solution p to (1), more precisely its even extension with respect to t, can be written as

$$p(\mathbf{x}, t) = (2\pi)^{-n} \int_{\mathbb{R}^n} \cos(t|\boldsymbol{\xi}|) e^{i\mathbf{x}\cdot\boldsymbol{\xi}} \mathcal{F}\{f\}(\boldsymbol{\xi}) \mathrm{d}\boldsymbol{\xi}, \quad \text{for} \quad (\mathbf{x}, t) \in \mathbb{R}^n \times \mathbb{R}. \tag{4}$$

Furthermore, we use expansions into spherical harmonics for the measurement data g and the Fourier transform of the initial pressure $\mathcal{F}f$, given by

$$g(\boldsymbol{\theta}, t) = \sum_{l=0}^{\infty} \sum_{k=0}^{N(n,l)} g_{lk}(t) Y_{lk}(\boldsymbol{\theta}) \tag{5}$$

$$\mathcal{F}\{f\}(\lambda\boldsymbol{\omega}) = \sum_{l=0}^{\infty} \sum_{k=0}^{N(n,l)} \mathcal{F}\{f\}_{lk}(\lambda) Y_{lk}(\boldsymbol{\omega}), \tag{6}$$

where $(\lambda, \boldsymbol{\omega}) \in [0,\infty) \times S^{n-1}$ with $\boldsymbol{\xi} = \lambda\boldsymbol{\omega}$.

Lemma 1. *Let $f \in C_0^\infty(B_{r_0})$ be the initial pressure distribution in system (1) and let g be the corresponding measurement data given by (3). Then for $\lambda > 0$ the*

equation

$$\mathcal{C}\left\{g_{lk}\right\}(\lambda) = (2\pi)^{-\frac{n}{2}}\pi 2^{-1} i^l \mathcal{F}\left\{f\right\}_{lk}(\lambda) \\ \times \left[(c_1 + c_2 l)\lambda^{\frac{n}{2}} J_{l+\frac{n-2}{2}}(\lambda) - c_2 \lambda^{\frac{n}{2}+1} J_{l+\frac{n}{2}}(\lambda)\right] \quad (7)$$

holds.

Proof. From the representation (4) of the pressure, we obtain

$$\boldsymbol{\theta} \bullet \nabla_{\mathrm{x}} p(\mathrm{x}, t) = (2\pi)^{-n} \int_{\mathbb{R}^n} (i\boldsymbol{\theta} \bullet \boldsymbol{\xi}) \cos(t|\boldsymbol{\xi}|) e^{i\mathrm{x}\cdot\boldsymbol{\xi}} \mathcal{F}\left\{f\right\}(\boldsymbol{\xi}) \mathrm{d}\boldsymbol{\xi}, \quad \text{for} \quad (\mathrm{x}, t) \in \mathbb{R}^n \times \mathbb{R}.$$

Change to spherical coordinates, $\boldsymbol{\xi} \to \lambda\boldsymbol{\omega}$, we can write direction dependent measurements as

$$\begin{aligned} g(\boldsymbol{\theta}, t) &= (2\pi)^{-n} \int_{S^{n-1}} \int_0^\infty [c_1 + c_2(i\boldsymbol{\theta} \bullet \boldsymbol{\xi})] \cos(t\lambda) e^{i\lambda\boldsymbol{\theta}\cdot\boldsymbol{\omega}} \mathcal{F}\left\{f\right\}(\lambda\boldsymbol{\omega}) \lambda^{n-1} \mathrm{d}\lambda \mathrm{d}S(\boldsymbol{\omega}) \\ &= (2\pi)^{-n} \int_{S^{n-1}} \int_0^\infty \left(c_1 e^{i\lambda\boldsymbol{\theta}\cdot\boldsymbol{\omega}} + c_2 \lambda \left(\partial_\lambda e^{i\lambda\boldsymbol{\theta}\cdot\boldsymbol{\omega}}\right)\right) \cos(t\lambda) \mathcal{F}\left\{f\right\}(\lambda\boldsymbol{\omega}) \lambda^{n-1} \mathrm{d}\lambda \mathrm{d}S(\boldsymbol{\omega}) \end{aligned}$$

With the expansions into spherical harmonics [22] this can be further computed to

$$g(\boldsymbol{\theta}, t) = (2\pi)^{-n} \sum_{l=0}^{\infty} \sum_{k=0}^{N(n,l)} \int_0^\infty \cos(t\lambda) \mathcal{F}\left\{f\right\}_{lk}(\lambda) \lambda^{n-1} \left(c_1 A_{lk} + c_2 B_{lk}\right) \mathrm{d}\lambda, \quad (8)$$

where we used the abbreviations

$$\begin{aligned} A_{lk} &= \int_{S^{n-1}} e^{i\lambda\boldsymbol{\theta}\cdot\boldsymbol{\omega}} Y_{lk}(\boldsymbol{\omega}) \mathrm{d}S(\boldsymbol{\omega}) \\ B_{lk} &= \lambda \left(\partial_\lambda \int_{S^{n-1}} e^{i\lambda\boldsymbol{\theta}\cdot\boldsymbol{\omega}} Y_{lk}(\boldsymbol{\omega}) \mathrm{d}S(\boldsymbol{\omega})\right). \end{aligned}$$

In order to compute the inner integral in (8), we use the identity (see, e.g. [23])

$$\int_{S^{n-1}} e^{i\lambda\boldsymbol{\theta}\cdot\boldsymbol{\omega}} Y_{lk}(\boldsymbol{\omega}) \mathrm{d}S(\boldsymbol{\omega}) = (2\pi)^{\frac{n}{2}} i^l \lambda^{\frac{2-n}{2}} J_{l+\frac{n-2}{2}}(\lambda) Y_{lk}(\boldsymbol{\theta}) \quad (9)$$

which further gives for the derivative

$$\partial_\lambda \left(\int_{S^{n-1}} e^{i\lambda\boldsymbol{\theta}\cdot\boldsymbol{\omega}} Y_{lk}(\boldsymbol{\omega}) \mathrm{d}S(\boldsymbol{\omega})\right) = (2\pi)^{\frac{n}{2}} i^l Y_{lk}(\boldsymbol{\theta}) \partial_\lambda \left([\lambda^{-\frac{n-2}{2}} J_{l+\frac{n-2}{2}}(\lambda)\right). \quad (10)$$

Moreover we need the identity (see, e.g. [24]) $\partial_\lambda[\lambda^{-\nu} J_\nu(\lambda)] = -\lambda^{-\nu} J_{\nu+1}(\lambda)$, which yields

$$\partial_\lambda \left(\lambda^l \lambda^{-l-\frac{n-2}{2}} J_{l+\frac{n-2}{2}}(\lambda)\right) = l\lambda^{-\frac{n}{2}} J_{l+\frac{n-2}{2}}(\lambda) - \lambda^{-\frac{n-2}{2}} J_{l+\frac{n-2}{2}}(\lambda).$$

Thus combining (9) and (10) we have

$$g(\boldsymbol{\theta},t)=(2\pi)^{-n/2}\sum_{l=0}^{\infty}\sum_{k=0}^{N(n,l)} i^l \int_0^{\infty}\cos(t\lambda)\mathcal{F}\left\{f\right\}_{lk}(\lambda)\lambda^{\frac{n}{2}}\left((c_1+c_2 l)J_{l+\frac{n-2}{2}}(\lambda)-c_2\lambda J_{l+\frac{n}{2}}(\lambda)\right). \tag{11}$$

Together with (5) we conclude that

$$g_{lk}(t)=(2\pi)^{-n/2} i^l \int_0^{\infty}\cos(t\lambda)\mathcal{F}\left\{f\right\}_{lk}(\lambda)\lambda^{\frac{n}{2}}\left((c_1+c_2 l)J_{l+\frac{n-2}{2}}(\lambda)-c_2\lambda J_{l+\frac{n}{2}}(\lambda)\right)\mathrm{d}\lambda,$$

which is equivalent to (7) and thus proves the Lemma. □

To obtain the proposed stable reconstruction formula, we investigate the coefficients $\mathcal{F}\left\{f\right\}_{lk}$ a bit further. Using equation (9) we have

$$\begin{aligned}
\mathcal{F}\left\{f\right\}_{lk}(\lambda) &= \int_{S^{n-1}}\int_{\mathbb{R}^n} e^{-i\lambda\mathbf{x}\cdot\boldsymbol{\omega}} f(\mathbf{x})\overline{Y_{lk}(\boldsymbol{\omega})}\mathrm{d}\mathbf{x}\mathrm{d}S(\boldsymbol{\omega}) \\
&= \int_{S^{n-1}}\int_0^{\infty} f(\rho\boldsymbol{\theta})\rho^{n-1}\left(\int_{S^{n-1}} e^{-i\lambda\rho\boldsymbol{\theta}\cdot\boldsymbol{\omega}}\overline{Y_{lk}(\boldsymbol{\omega})}\mathrm{d}S(\boldsymbol{\omega})\right)\mathrm{d}\rho\mathrm{d}S(\boldsymbol{\theta}) \\
&= \int_{S^{n-1}}\int_0^{\infty} f(\rho\boldsymbol{\theta})\rho^{n-1}\left(\overline{\int_{S^{n-1}} e^{i\lambda\rho\boldsymbol{\theta}\cdot\boldsymbol{\omega}} Y_{lk}(\boldsymbol{\omega})\mathrm{d}S(\boldsymbol{\omega})}\right)\mathrm{d}\rho\mathrm{d}S(\boldsymbol{\theta}) \\
&= (2\pi)^{\frac{n}{2}}\overline{i^l}\int_{S^{n-1}}\int_0^{\infty} f(\rho\boldsymbol{\theta})\rho^{\frac{n}{2}}\lambda^{\frac{2-n}{2}}J_{l+\frac{n-2}{2}}(\lambda\rho)\overline{Y_{lk}(\boldsymbol{\omega})}\mathrm{d}\rho\mathrm{d}S(\boldsymbol{\theta}).
\end{aligned}$$

This shows that $\mathcal{F}\left\{f\right\}_{lk}$ can be written as

$$\mathcal{F}\left\{f\right\}_{lk}(\lambda)=(2\pi)^{\frac{n}{2}}\overline{i^l}\lambda^{\frac{2-n}{2}}\int_0^{\infty} f_{lk}(\rho)\rho^{\frac{n}{2}}J_{l+\frac{n-2}{2}}(\lambda\rho)d\rho. \tag{12}$$

The latter computations together with Lemma 1 gives the following result.

Theorem 2. *Let $f\in C_0^{\infty}(B_{r_0})$ be the initial pressure distribution and let g be direction dependent measurement data* (3)*, then we have that*

$$f(\mathbf{x})=\frac{2}{\pi}\sum_{l=0}^{\infty}\sum_{k=0}^{N(n,l)}|\mathbf{x}|^{1-\frac{n}{2}}\int_0^{\infty}\frac{\mathcal{C}\left\{g_{lk}\right\}(\lambda)J_{l+\frac{n-2}{2}}(\lambda|\mathbf{x}|)\mathrm{d}\lambda}{(c_1+c_2 l)J_{l+\frac{n-2}{2}}(\lambda)-c_2\lambda J_{l+\frac{n}{2}}(\lambda)}Y_{lk}\left(\frac{\mathbf{x}}{|\mathbf{x}|}\right). \tag{13}$$

Proof. Combining Lemma 1 and (12) we have that

$$\int_0^{\infty} f_{lk}(\rho)\rho^{\frac{n}{2}}J_{l+\frac{n-2}{2}}(\lambda\rho)\mathrm{d}\rho=\frac{2}{\pi}\frac{\mathcal{C}\left\{g_{lk}\right\}(\lambda)}{(c_1+c_2 l)\lambda J_{l+\frac{n-2}{2}}(\lambda)-c_2\lambda^2 J_{l+\frac{n}{2}}(\lambda)},$$

where we used $i^l\bar{i^l} = |i| = 1$. We recognize that the left hand side is the Hankel transform of order $l + \frac{n-2}{2}$ of $f_{lk}(\rho)\rho^{\frac{n}{2}-1}$. Hence, applying the Hankel transform of order $l + \frac{n-2}{2}$, we obtain

$$f_{lk}(\rho) = \frac{2}{\pi}\rho^{1-\frac{n}{2}} \int_0^\infty \frac{\mathcal{C}\left\{g_{lk}\right\}(\lambda) J_{l+\frac{n-2}{2}}(\lambda\rho)\mathrm{d}\lambda}{(c_1 + c_2 l)J_{l+\frac{n-2}{2}}(\lambda) - c_2\lambda J_{l+\frac{n}{2}}(\lambda)},$$

which gives the desired result. □

In practice reconstructing the initial pressure by the inversion formula stated in Theorem 2 is unstable due to its zeros of the denominator. However, we are able to provide a stable inversion formula by using a Fourier Bessel series to evaluate the inner integral in formula (13).

3 Stable inversion formulas

Since in real situations only noisy data $g^\delta \in L^2\left(S_{r_0}^{n-1} \times [0,T]\right)$ are available the cosine transform $\mathcal{C}\left\{g_{lk}^\delta\right\}(\lambda)$ may not vanish at the roots of the denominator $(c_1 + c_2 l)J_{l+\frac{n-2}{2}}(\lambda) - c_2\lambda J_{l+\frac{n}{2}}(\lambda)$ in formula (13), which means that Theorem 2 can not be directly used to reconstruct initial pressure density f. However, we are able to avoid the zeros of the denominator by using a Fourier Bessel series expansion, which leads to a stable reconstruction of the initial pressure, similar as in [19, 21, 25].

Theorem 3. *Let $f \in C_0^\infty(B_{r_0})$ and assume that direction dependent data g are given by* (3)*. Then f can be reconstructed by*

$$f(\mathbf{x}) = -|\mathbf{x}|^{1-\frac{n}{2}}\frac{2^2}{\pi} \times \sum_{l=0}^{\infty}\sum_{k=0}^{N(n,l)}\sum_{j=1}^{\infty}\left(\frac{\mathcal{C}\left\{g_{lk}\right\}(w_{j,l+\frac{n-2}{2}})J_{l+\frac{n-2}{2}}(w_{j,l+\frac{n-2}{2}}\rho)}{c_2 w_{j,l+\frac{n-2}{2}}^2 J_{l+\frac{n}{2}}(w_{j,l+\frac{n-2}{2}})^3}\right) Y_{lk}\left(\frac{\mathbf{x}}{|\mathbf{x}|}\right), \quad (14)$$

where $w_{j,l+\frac{n-2}{2}}$ denotes the j-th positive zero of the l-th order Bessel function of the first kind $J_{l+\frac{n-2}{2}}$.

Proof. Since f_{lk} is of class C^∞ and is compactly supported, we can expand it into a Fourier Bessel series (see [24]) and it follows that

$$\begin{aligned} & f_{lk}(\rho)\rho^{\frac{n}{2}-1} \quad (15)\\ &= \sum_{j=1}^{\infty}\frac{2}{J_{l+\frac{n}{2}}(w_{j,l+\frac{n-2}{2}})^2}\int_0^\infty f_{lk}(r)J_{l+\frac{n-2}{2}}(w_{j,l+\frac{n-2}{2}}r)r^{\frac{n}{2}}\,\mathrm{d}r\; J_{l+\frac{n-2}{2}}(w_{j,l+\frac{n-2}{2}}\rho)\\ &= (2\pi)^{-\frac{n}{2}}\sum_{j=1}^{\infty}\frac{2}{J_{l+\frac{n}{2}}(w_{j,l+\frac{n-2}{2}})^2}\mathcal{F}\left\{f\right\}_{lk}(w_{j,l+\frac{n-2}{2}})w_{j,l+\frac{n-2}{2}}^{\frac{n-2}{2}}\overline{i^{-l}}\; J_{l+\frac{n-2}{2}}(w_{j,l+\frac{n-2}{2}}\rho), \end{aligned}$$

where in the last line, we used (12). From Lemma 1, we have

$$\mathcal{C}\left\{g_{lk}\right\}(w_{j,l+\frac{n-2}{2}}) = -(2\pi)^{-\frac{n}{2}}\pi 2^{-1} i^l \mathcal{F}\left\{f\right\}_{lk}(w_{j,l+\frac{n-2}{2}})c_2 w_{j,l+\frac{n-2}{2}}^{\frac{n}{2}+1} J_{l+\frac{n}{2}}(w_{j,l+\frac{n-2}{2}}).$$

Together with (15), we have

$$f_{lk}(\rho)\rho^{\frac{n}{2}-1} = -\sum_{j=1}^{\infty} \frac{2^2}{\pi} \frac{\mathcal{C}\left\{g_{lk}\right\}\left(w_{j,l+\frac{n-2}{2}}\right) J_{l+\frac{n-2}{2}}\left(w_{j,l+\frac{n-2}{2}}\rho\right)}{c_2 w_{j,l+\frac{n-2}{2}}^2 J_{l+\frac{n}{2}}\left(w_{j,l+\frac{n-2}{2}}\right)^3},$$

which concludes the proof. □

Numerical examples in section 5 will be based on an implementation of the series (14). They indicate that (14) provides a stable reconstruction formula.

4 Inversion from weighted spherical means

In this section we derive an inversion formula for the following weighted spherical mean transform

$$M_{\cos} f(\boldsymbol{\theta}, r) = \frac{1}{|S^{n-1}|} \int_{S^{n-1}} f(\mathbf{x} + r\boldsymbol{\omega})(\boldsymbol{\theta} \cdot \boldsymbol{\omega}) \mathrm{d}S(\boldsymbol{\omega}), \quad (\boldsymbol{\theta}, t) \in S^{n-1} \times (0, \infty). \tag{16}$$

Note that the weight $\boldsymbol{\theta} \cdot \boldsymbol{\omega}$ is the cosine of the angle between $\boldsymbol{\theta}$ and $\boldsymbol{\omega}$. To derive the inversion formula we will express the normal derivative of the acoustic pressure in terms of the weighted spherical means. Such a relation can also be used for numerically solving the forward problem in PAT with direction dependent data.

It is well known (see [21, 22]) that a solution p of system (1) can be written as

$$p(\mathbf{x}, t) = \begin{cases} \frac{\sqrt{\pi}}{\Gamma(n/2)} t D_t^{\frac{n-1}{2}} (t^{n-2} M f(\mathbf{x}, t)) & \text{if } n \text{ is odd} \\ \frac{2}{\Gamma(n/2)} t D_t^{\frac{n}{2}} \int_0^t \frac{r^{n-1} M f(\mathbf{x}, r)}{\sqrt{t^2 - r^2}} \mathrm{d}r & \text{if } n \text{ is even,} \end{cases} \tag{17}$$

where $(D_t f)(t) := \frac{1}{2t} \frac{\partial f}{\partial t}$ and Mf denotes the spherical Radon transform given by

$$Mf(\mathbf{x}, r) = \frac{1}{|S^{n-1}|} \int_{S^{n-1}} f(\mathbf{x} + r\boldsymbol{\omega}) \mathrm{d}S(\boldsymbol{\omega}), \quad (\mathbf{x}, t) \in \mathbb{R}^n \times \mathbb{R}.$$

In the following we establish an analogous results direction dependent, which states that they can be computed from the weighted spherical Radon transform.

Lemma 4. *Assume p is a solution to system* (1)*. Then the normal derivative of acoustic pressure is given by*

$$\boldsymbol{\theta} \cdot \nabla_{\mathbf{x}} p(\mathbf{x}, t)|_{\mathbf{x}=\boldsymbol{\theta}} = \begin{cases} \frac{\sqrt{\pi}}{\Gamma(n/2)} t D_t^{\frac{n-1}{2}} \left(t^{n-2} \partial_t M_{\cos} f(\mathbf{x}, t)\right) & \textit{if } n \textit{ is odd} \\ \frac{2}{\Gamma(n/2)} t D_t^{\frac{n}{2}} \int_0^t \frac{r^{n-1} \partial_r M_{\cos} f(\mathbf{x}, r)}{\sqrt{t^2 - r^2}} dr & \textit{if } n \textit{ is even} \end{cases}. \tag{18}$$

Proof. By formula (17) we have

$$\boldsymbol{\theta} \cdot \nabla_{\mathbf{x}} p(\mathbf{x}, t)|_{\mathbf{x}=\boldsymbol{\theta}} = \begin{cases} \dfrac{\sqrt{\pi}}{\Gamma(n/2)} t D_t^{\frac{n-1}{2}} (t^{n-2} \boldsymbol{\theta} \cdot \nabla_{\mathbf{x}} (Mf)(\mathbf{x}, t)|_{\mathbf{x}=\boldsymbol{\theta}}) & \text{if } n \text{ is odd} \\ \dfrac{2}{\Gamma(n/2)} t D_t^{\frac{n}{2}} \displaystyle\int_0^t \frac{r^{n-1} \boldsymbol{\theta} \cdot \nabla_{\mathbf{x}} (Mf)(\mathbf{x}, r)|_{\mathbf{x}=\boldsymbol{\theta}}}{\sqrt{t^2 - r^2}} \mathrm{d}r & \text{if } n \text{ is even.} \end{cases}$$

A simple computation shows

$$\begin{aligned} \boldsymbol{\theta} \cdot \nabla_{\mathbf{x}} (Mf)(\mathbf{x}, r)|_{\mathbf{x}=\boldsymbol{\theta}} &= \frac{1}{|S^{n-1}|} \int_{S^{n-1}} \boldsymbol{\theta} \cdot \nabla_{\mathbf{x}} f(\mathbf{x} + r\boldsymbol{\omega})|_{\mathbf{x}=\boldsymbol{\theta}} \mathrm{d}S(\boldsymbol{\omega}) \\ &= \frac{1}{|S^{n-1}|} \int_{S^{n-1}} \partial_r f(\boldsymbol{\theta} + r\boldsymbol{\omega})(\boldsymbol{\theta} \cdot \boldsymbol{\omega}) \mathrm{d}S(\boldsymbol{\omega}) = \partial_r M_{\cos} f(\boldsymbol{\theta}, r), \end{aligned}$$

and concludes the proof. □

The above lemma immediately implies the following.

Theorem 5. *Any function $f \in C_0^\infty(B_{r_0})$ can be recovered from the weighted spherical means $M_{\cos} f$ in* (16) *by first recovering $\boldsymbol{\theta} \cdot \nabla_{\mathbf{x}} p$ with* (18) *and subsequently applying formula* (13)*.*

Simplifying the combination of (18) and (13) is an interesting line of future research.

5 Numerical experiments

We will derive reconstructions for direction dependent data based on the frequency domain formula derived in section 3 for the case $n = 2$. We will present reconstructions for direction dependent data for $c_1 = c_2 = 1$. The results show that PAT with direction dependent data yields to accurate reconstructions.

5.1 Discretization and data simulation

In numerical experiments we simulate direction dependent measurement data on a circle of radius R, which arises in applications when acoustic pressure is measured by integrating line detectors on a cylinder [26]. In order to compute the pressure field and its gradient restricted to the circle we use a discrete wave propagation model in this work. For that purpose we implement wave propagation on a 2D quadratic grid with side lenght a. Its nodes are given by

$$\mathbf{x}_{i_1, i_2} := -(a, a) + \frac{2a}{N} \quad \text{for } (i_1, i_2) \in \{0, \dots, N-1\}$$

as depicted in Figure 2. As in [4], we compute the solution to (1) by the k-space method [27, 28], since it is an accurate model for wave propagation that does not suffer from frequency dependent dispersion. Numerically the parameter b has to be

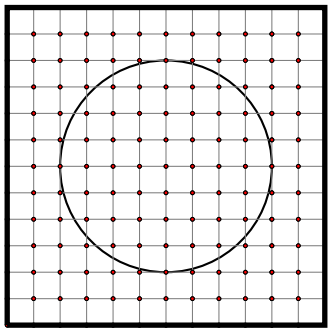

Figure 2: Discrete acoustic wave propagation is computed on a 2D quadratic grid to simulate direction dependent data.

chosen large enough to contain the discretized initial pressure f and the acoustic field $p(\cdot, T)$.

Then we obtain the values of the acoustic pressure field and its gradient on the circle by linear interpolation, computed by the standard MATLAB routine. Figure 3 shows the

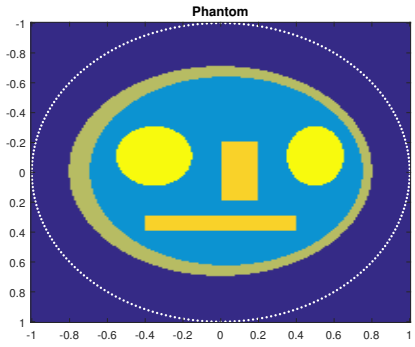

Figure 3: The image shows an artificial pressure distribution inside a sphere, which boundary is indicated by the white dots.

artificial initial pressure distribution, which is the source of our propagating wave. In Figure 4 direction dependent measurement data for the case $c_1 = c_2 = 1$ are compared to classical measurement data, which correspond to the case $c_1 = 1, c_2 = 0$.

5.2 Application of the discrete reconstruction series and results

In order to reconstruct the initial pressure distribution, we implement a discrete version of reconstruction formula (14), which for the case $n = 2$ reads as

$$f(\mathbf{x}) = -\frac{4}{\pi} \sum_{k \in \mathbb{Z}} \sum_{j=1}^{\infty} \frac{\mathcal{C}\left\{g_k\right\}\left(\omega_{j,k}\right) J_k\left(\omega_{j,k}\rho\right)}{c_2 \omega_{j,k}^2 J_{k+1}\left(\omega_{j,k} R\right)^3} e^{ik\varphi}. \tag{19}$$

The inversion formula (19) has been implemented following similar formula in [18] for standard PAT data. The initial pressure (3) is given on a 200×200 grid and the pressure data are simulated for 300 sensor locations.

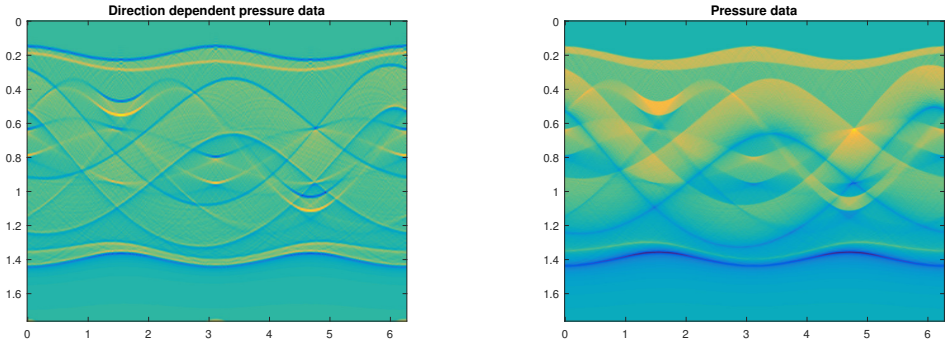

Figure 4: Pressure data for PAT as function of time (vertical axis) and detector position (horizontal axis). Left: Direction dependent data for the case $c_1 = c_2 = 1$. Right: Classical measurement data $c_1 = 1$ and $c_2 = 0$.

Reconstruction results from exact data and for noisy data (additive Gaussian noise with relative ℓ^2 data error of 0.0023) are shown in Figure 5.

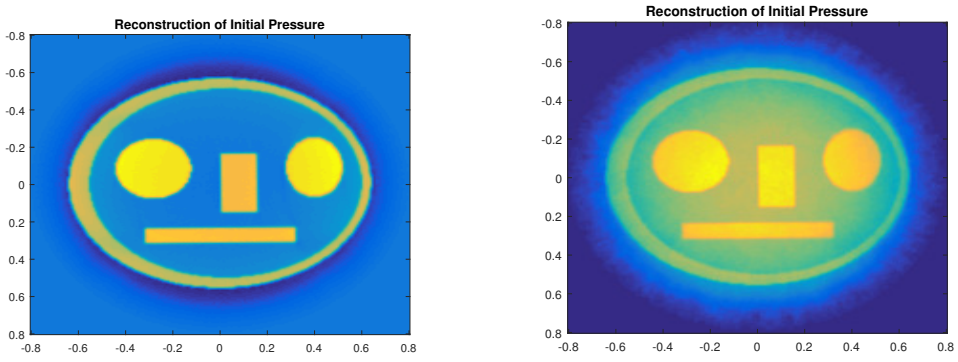

Figure 5: Left: Reconstruction of the initial pressure from simulated data. Right: Reconstruction from noisy data with a relative ℓ^2-data error of 0.0023.

6 Conclusion

We investigated PAT direction dependent data, which uses a linear combination of the acoustic pressure and its normal derivative. We developed a reconstruction formula for the special case of spherical detection geometry and derived an exact reconstruction formula. Numerical results that show validity of the proposed approach. It is an interesting line of future research to investigate the direction dependent data model for general detection geometries in PAT and for variable speed of sound wave propagation.

Acknowledgments

The work of G.Z. and M.H. has been supported by the Austrian Science Fund (FWF), project P 30747-N32. The work of S.M. has been supported by the National Research Foundation of Korea grant funded by the Korea government (MSIP) (NRF-2018R1D1A3B07041149).

References

[1] Yuan Xu and Lihong Wang. Time reversal and its application to tomography with diffracting sources. *Physical review letters*, 92(3):033902, 2004.

[2] David Finch. On a thermoacoustic transform. *Proc. 8th Int. Meeting on Fully 3D Image Reconstruction in Radiology and Nuclear Medicine*, pages 150–151, 2005.

[3] Guenther Paltauf, Petra Hartmair, Georgi Kovachev, and Robert Nuster. Piezoelectric line detector array for photoacoustic tomography. *Photoacoustics*, 8:28–36, 2017.

[4] Markus Haltmeier and Linh Nguyen. Analysis of iterative methods in photoacoustic tomography with variable sound speed. *SIAM Journal on Imaging Sciences*, 10(2):751–781, 2017.

[5] Peter Kuchment and Leonid Kunyansky. Mathematics of thermoacoustic tomography. *European Journal of Applied Mathematics*, 19(2):191–224, 2008.

[6] Leonid Kunyansky. Thermoacoustic tomography with detectors on an open curve: an efficient reconstruction algorithm. *Inverse Problems*, 24(5):055021, 2008.

[7] Zakaria Belhachmi, Thomas Glatz, and Otmar Scherzer. A direct method for photoacoustic tomography with inhomogeneous sound speed. *Inverse Problems*, 32(4):045005, 2016.

[8] Plamen Stefanov and Gunther Uhlmann. Thermoacoustic tomography with variable sound speed. *Inverse Problems*, 25(7):075011, 2009.

[9] Leonid Kunyansky. Reconstruction of a function from its spherical (circular) means with the centers lying on the surface of certain polygons and polyhedra. *Inverse Problems*, 27(2):025012, 2011.

[10] Leonid Kunyansky. Inversion of the spherical means transform in corner-like domains by reduction to the classical radon transform. *Inverse Problems*, 31(9):095001, 2015.

[11] Markus Haltmeier. Universal inversion formulas for recovering a function from spherical means. *SIAM Journal on Mathematical Analysis*, 46(1):214–232, 2014.

[12] Markus Haltmeier. Inversion of circular means and the wave equation on convex planar domains. *Computers & Mathematics with Applications. An International Journal*, 65(7):1025–1036, 2013.

[13] Linh Nguyen. A family of inversion formulas in thermoacoustic tomography. *Inverse Problems and Imaging*, 3(4):649–675, 2009.

[14] David Finch, Sarah Patch, and Rakesh. Determining a function from its mean values over a family of spheres. *SIAM journal on mathematical analysis*, 35(5):1213–1240, 2004.

[15] Frank Natterer. Photo-acoustic inversion in convex domains. *Inverse Problems Imaging*, 2012.

[16] Viktor Palamodov. A uniform reconstruction formula in integral geometry. *Inverse Probl.*, 28(6):065014, 2012.

[17] Mark Agranovsky and Peter Kuchment. Uniqueness of reconstruction and an inversion procedure for thermoacoustic and photoacoustic tomography with variable sound speed. *Inverse Problems*, 23(5):2089, 2007.

[18] Markus Haltmeier. Frequency domain reconstruction for photo-and thermoacoustic tomography with line detectors. *Mathematical Models and Methods in Applied Sciences*, 19(02):283–306, 2009.

[19] Gerhard Zangerl, Otmar Scherzer, and Markus Haltmeier. Exact series reconstruction in photoacoustic tomography with circular integrating detectors. *Communications in Mathematical Sciences*, 7(3):665–678, 2009.

[20] Leonid Kunyansky. A series solution and a fast algorithm for the inversion of the spherical mean radon transform. *Inverse Problems*, 23(6):S11, 2007.

[21] Markus Haltmeier, Otmar Scherzer, Peter Burgholzer, Robert Nuster, and Guenther Paltauf. Thermoacoustic tomography and the circular radon transform: exact inversion formula. *Mathematical Models and Methods in Applied Sciences*, 17(04):635–655, 2007.

[22] David Finch. The spherical mean value operator with centers on a sphere. *Inverse Problems*, 23(6):S37, 2007.

[23] Frank Natterer. *The mathematics of computerized tomography*, volume 32. Siam, 1986.

[24] Gerald Folland. *Fourier analysis and its applications*, volume 4. American Mathematical Soc., 2009.

[25] Gerhard Zangerl and Otmar Scherzer. Exact reconstruction in photoacoustic tomography with circular integrating detectors ii: Spherical geometry. *Mathematical Methods in the Applied Sciences*, 33(15):1771–1782, 2010.

[26] Peter Burgholzer, Johannes Bauer-Marschallinger, Hubert Grün, Markus Haltmeier, and Günther Paltauf. Temporal back-projection algorithms for photoacoustic tomography with integrating line detectors. *Inverse Problems*, 23(6):S65, 2007.

[27] Benjamin Cox, Kara Schvartz-Leyzac Kara, Simon Arridge, and Paul Beard. k-space propagation models for acoustically heterogeneous media: Application to biomedical photoacoustics. *The Journal of the Acoustical Society of America*, 121(6):3453–3464, 2007.

[28] Douglas Mast, Laurent Souriau, Donald Liu, Makoto Tabei, Adrian Nachman, and Robert Waag. A k-space method for large-scale models of wave propagation in tissue. *IEEE transactions on ultrasonics, ferroelectrics, and frequency control*, 48(2):341–354, 2001.